ORGANOMETALLICS

Article

pubs.acs.org/Organometallics

β-Oxo-δ-diimine Nickel Complexes: A Comparison of Tautomeric Active Species in Ethylene Polymerization Catalysis

Hsin-Chun Chiu, Adam J. Pearce, Peter L. Dunn, Christopher J. Cramer, and Ian A. Tonks*

Department of Chemistry, University of Minnesota−Twin Cities, 207 Pleasant Street SE, Minneapolis, Minnesota 55455, United States

Supporting Information

ABSTRACT: A series of mono- and bimetallic Ni alkyl complexes of a β-oxo-δ-diimine (BODDI) ligand are reported. The monometallic complexes have a second binding pocket, of which the free "arm" can exist as either an enamine (e.g., **8**, BODEI, β-oxo-δ-enamineiminato) or imine (e.g., **3**, BODII, β-oxo-δ-imineiminato) tautomer. The identity of the tautomer in the secondary Ni coordination sphere has a significant effect on ethylene polymerization behavior: the enamine tautomer, which hydrogen bonds to the central O atom and is in conjugation with the N,O backbone chelate, is significantly more electron rich and yields a much lower molecular weight polymer than the imine tautomer, which rotates away from Ni to a distal position and has little effect on polymerization. Deprotonation of the second binding pocket with M(HMDS) (M = Li, Na, K) yields the Ni-alkali metal heterobimetallic complexes **3Li**, **3Na**, and **3K**. The deprotonated alkali metal enamides display ethylene polymerization behavior similar to the neutral imine complex because the enamide arm can also distally rotate to minimize interaction with the Ni coordination sphere upon activation.

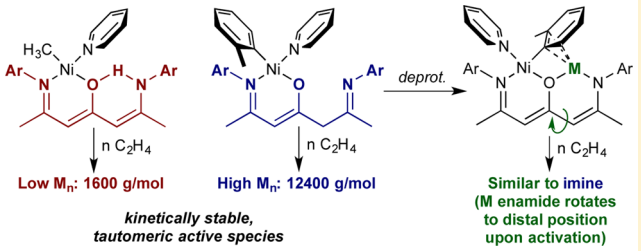

INTRODUCTION

Late transition metal catalysts have been widely employed in ethylene polymerization catalysis and polar comonomer ethylene copolymerization catalysis due to their functional group tolerance.[1] The majority of functional comonomer polymerization reactions have utilized either Brookhart-type α-diimine[2] or Drent-type phosphine sulfonate[3] ligands, indicating an opportunity for continued catalysis advancement through the design of new ligand sets with new metal−ligand interactions.

Akin to this, recent progress has seen several elegant examples that utilize secondary coordination sphere interactions[4] to affect various aspects of ethylene homo- and copolymerization catalysis. For example, Jordan and Bazan have each demonstrated that coordination of exogenous Lewis acids to ligands on group 10 polymerization catalysts can drastically impact polymerization activities, molecular weight distributions, and comonomer incorporation.[5] Similarly, Do recently reported on the effects of installing alkali metal cations into the secondary coordination sphere of phenoxyiminato Ni ethylene polymerization catalysts.[6] Through prudent alkali metal choice, Do was able to observe up to 20-fold increases in catalytic rates as well as significant enhancement of polymer molecular weight and branching. Transition metal bimetallic effects have also been observed; for example, Agapie reported the copolymerization of ethylene and amino olefins catalyzed by homobimetallic dinickel complexes.[7] Tethered heteroatoms usually inhibit olefin polymerization through the formation of stable chelate rings, but addition of a bulky second metal site in the secondary coordination sphere of Ni prevents stable chelate formation. Other bimetallic Fe, Ni, Cu, and early transition metal systems have shown similar cooperative effects, where addition of a second metal impacts the overall molecular weight, activity, and comonomer incorporation.[8] Secondary coordination sphere effects have also played an important role in the design and development of many inorganic systems for small-molecule activation and enzyme active site models.[9]

Given the significant secondary coordination sphere effects observed in late transition metal polymerization catalysis, we are interested in engineering bimetallic polymerization catalysts that contain one-atom bridges between the two metal centers to further enhance stereoelectronic effects. Such catalysts may also mimic the effects of bridging anions/activators found in many catalytic systems.[10] Herein, we report the synthesis, characterization, and ethylene polymerization activity of a series of mono- and bimetallic Ni-alkali metal complexes ligated by a β-oxo-δ-diiminate ligand, which has previously been used for the synthesis of several homobimetallic dizinc and dilutetium complexes.[11]

MATERIALS AND METHODS

General Materials, Considerations, and Instrumentation. All air- and moisture-sensitive compounds were manipulated in a glovebox under a nitrogen atmosphere. All solvents were dried in a Glass Contour solvent system, and liquid reagents were passed through activated basic alumina and titrated with a stock solution of Na/

Received: March 30, 2016

DOI: 10.1021/acs.organomet.6b00256
Organometallics XXXX, XXX, XXX−XXX

benzophenone where compatible to ensure dryness. Ultra-high-purity ethylene (99.9%) was purchased from Airgas, and oxygen and water were further removed by using a PUR-Gas in-line purifier system from Matheson. Diacetylacetone,[11a] (tmeda)Ni(*o*-tolyl)Cl,[12] $[(\eta^3\text{-}C_3H_5)\text{-}NiBr]_2$,[13] $(PMe_3)Ni(\eta^3\text{-}C_7H_7)Cl$,[14] $Ni(\eta^3\text{-methallyl})_2$,[15] (tmeda)-$NiMe_2$,[16] and *β*-ket(2,6-diisopropylphenyl)imine (BKI)[17] were prepared according to literature procedures.

^1H and ^{13}C spectra of ligand and complexes were collected on Bruker Avance III HD NanoBay 400 MHz, Bruker Avance III HD 500 MHz, or Varian Inova 500 MHz spectrometers. ^{13}C spectra of polyethylene were collected at 100 °C in 1,1,2,2-tetrachloroethane on an Agilent/Varian VNMR 600 MHz spectrometer. X-ray crystallography was collected on a Bruker APEX II CCD diffractometer with a 0.710 73 Å Mo K*α* source or on a Bruker-AXS D8 Venture diffractometer with a 1.541 78 Å Cu K*α* source. GPC analyses were carried out on an Agilent PL-GPC 220 high-temperature GPC/SEC system at 135 °C in 1,2,4-trichlorobenzene calibrated with polystyrene standards with a universal correction for linear polyethylene in the Mark−Houwink equation (K = 39.0 mL/mg, α = 0.729).[18] Differential scanning calorimetry (DSC) analyses were carried out on a TA Discovery DSC system.

General Polymerization. All polymerization reactions were carried out in a Biotage Endeavor parallel pressure reactor with overhead stirring housed in a N_2 atmosphere glovebox. A toluene stock solution of catalyst was diluted in the reactor. Reactions were run with 2 mL total reaction volume in toluene or THF at catalyst concentrations of 0.2 mM. Polymerizations with additives were run with 500 equiv of triethylamine or 1 equiv of the appropriate crown ether. Then, the reactor was sealed, heated (36 °C), and pressurized with C_2H_4 (30 atm). The reactions were run for 3 h. Afterward, the reactions were depressurized and removed from the glovebox, and the polymer was precipitated out by the addition of acetone, filtered, and dried *in vacuo* prior to analysis by NMR, gel permeation chromatography (GPC), and DSC.

X-ray Crystal Data: General Procedure. Crystals were removed quickly from a scintillation vial to a microscope slide coated with paraffin oil. Samples were selected and mounted on the tip of a 0.1 mm diameter glass capillary. The structures were solved by direct methods. All non-hydrogen atoms were refined anisotropically. Details regarding refined data and cell parameters are available in Tables S1 and S2 in the Supporting Information.

*Synthesis of $C_{31}H_{44}N_2O$, H(BODDI) (**1**).* The preparation of this ligand followed the published procedure with a slight modification.[11a] A mixture of diacetylacetone (801 mg 5.63 mmol) and 2,6-diisopropylaniline (2.99 g, 16.8 mmol) was stirred for 3 days. The solution turned to an orange-brown solid, at which point 5 mL of ethanol was added and the solution was sonicated. Addition of 15 mL of deionized water caused a pale yellow powder to precipitate. The suspension was filtered, washed with water, and dried *in vacuo* to yield **1** (2.21 g, 85.2% yield). Both ^1H and ^{13}C NMR spectra match the reported values.

*Synthesis of $C_{31}H_{43}N_2OK$, H(BODII)K (**2**).* To a solution of **1** (921 mg, 2.0 mmol) in THF (3 mL) was added dropwise a solution of ^{t}BuOK (258 mg, 2.3 mmol) in THF (2 mL) at ambient temperature. After the color of the mixture turned light yellow, the mixture was stirred for another 1 h. The volatiles were removed *in vacuo*, and then the crude product was triturated in 5 mL of hexanes overnight. **2** was collected via vacuum filtration as a white powder (850 mg, 85% yield). ^1H NMR (CD_2Cl_2, 400 MHz): δ 7.13 (m, 6H), 4.76 (s, 1H), 3.09 (s, 2H), 2.96 (sep, 2H, J = 6.8 Hz), 2.79 (sep, 2H, J = 6.8 Hz), 1.88 (s, 3H), 1.55 (s, 3H), 1.16 (m, 12H), 0.92 (d, 6H, J = 6.9 Hz) ppm.

*Synthesis of $C_{43}H_{55}N_3ONi$, H(BODII)Ni(o-tolyl)(py) (**3**).* A solution of (tmeda)Ni(*o*-tolyl)Cl (30.6 mg, 0.1 mmol) and pyridine (30.0 *μ*L, 1.5 mmol) in benzene (3 mL) was added to a suspension of deprotonated ligand **2** (49.9 mg, 0.1 mmol) in benzene (2 mL) at ambient temperature. The suspension became an orange solution, and within 30 min KCl precipitation was evident. The mixture was stirred at ambient temperature for 1.5 h and then filtered to collect the filtrate. Volatiles of the filtrate were removed *in vacuo* to yield an orange solid. The crude product was dissolved in minimal pentane, and large X-ray quality orange crystals of **3** were obtained from slow evaporation of the solvent (30.0 mg, 44% yield). ^1H NMR (C_6D_6, 500 MHz): δ 8.54 (d, 2H, $^3J_{HH}$ = 6.0 Hz), 7.27 (d, 1H, $^3J_{HH}$ = 7.4 Hz), 7.18−7.08 (m, 4H), 6.74 (d, 1H, $^3J_{HH}$ = 7.5 Hz), 6.59−6.56 (m, 3H), 6.50 (br, 1H), 6.41 (t, 1H, $^3J_{HH}$ = 7.5 Hz), 6.10 (d, 2H, $^3J_{HH}$ = 6.5 Hz), 5.36 (d, 1H, $^4J_{HH}$ = 1.2 Hz), 4.72 (sep, 1H, $^3J_{HH}$ = 6.5 Hz), 3.74 (s, 3H), 3.48 (d, 1H, $^2J_{HH}$ = 12.4 Hz), 3.37 (d, 1H, $^2J_{HH}$ = 12.1 Hz), 2.85−3.11 (m, 2H), 2.79 (sep, 1H, $^3J_{HH}$ = 6.3 Hz), 2.32 (d, 3H, $^3J_{HH}$ = 6.4 Hz), 1.64 (s, 3H), 1.50 (d, 3H, $^4J_{HH}$ = 1.2 Hz), 1.28−1.24 (m, 6H), 1.21 (d, 3H, $^3J_{HH}$ = 6.9 Hz), 1.18 (d, 3H, $^3J_{HH}$ = 7.0 Hz), 1.09 (d, 3H, $^3J_{HH}$ = 6.5 Hz), 1.03 (d, 3H, $^3J_{HH}$ = 6.8 Hz), 0.47 (d, 3H, $^3J_{HH}$ = 5.8 Hz) ppm. $^{13}C\{^1H\}$ NMR (C_6D_6, 125 MHz): δ 174.38 (O−C), 167.47 (N═C), 167.38 (N═C), 151.79, 151.63, 150.52, 147.82, 146.84, 143.30, 141.27, 140.91, 136.31, 136.10, 135.71, 135.41, 125.45, 123.39, 123.30, 123.03, 122.93, 122.86, 122.39, 121.93, 99.54 (═*β*C), 52.73 (−*β*C), 28.82, 28.03, 27.92, 27.70, 25.24, 24.61, 24.37, 24.17, 23.30, 23.16, 22.94, 22.88, 22.78, 19.36 ppm. Anal. Calcd (%) for $C_{43}H_{55}N_3ONi$: C, 75.00; H, 8.05; N, 6.10. Found: C, 73.05; H, 7.85; N, 5.29.

*Synthesis of $C_{34}H_{48}N_2ONi$, H(BODII)Ni(η^3-C_3H_5) (**4i**).* A solution of $[(\eta^3\text{-}C_3H_5)NiBr]_2$ (36.0 mg, 0.1 mmol) in Et_2O (2 mL) was added dropwise to a suspension of the deprotonated ligand **2** (101.0 mg, 0.2 mmol) in Et_2O (2 mL) at ambient temperature. The suspension became an orange solution, and within 30 min KCl precipitation was evident. The mixture was stirred at ambient temperature for 1 h and then filtered to collect the filtrate. Volatiles of the filtrate were removed *in vacuo* to yield an orange-yellow solid. The crude product was dissolved in minimal pentane, and large X-ray quality brown crystals of **4** were obtained from slow evaporation of the solvent (64.2 mg, 58% yield). ^1H NMR (C_6D_6, 500 MHz): δ 7.20 (br, 1H), 7.14−7.09 (m, 2H), 7.02−6.96 (m, 3H), 5.65−5.58 (m, 1H), 5.29 (s, 1H), 3.84 (sep, 1H, $^3J_{HH}$ = 7.0 Hz), 3.42 (s, 2H), 3.21 (sep, 1H, $^3J_{HH}$ = 7.0 Hz), 3.12−3.01 (m, 3H), 2.56 (d, 1H, $^3J_{HH}$ = 13.0 Hz), 1.70 (s, 3H), 1.46 (s, 3H), 1.42 (d, 1H, $^3J_{HH}$ = 13.0 Hz), 1.29 (d, 3H, $^3J_{HH}$ = 6.5 Hz), 1.28 (d, 3H, $^3J_{HH}$ = 6.5 Hz), 1.28 (d, 3H, $^3J_{HH}$ = 6.5 Hz), 1.26 (d, 6H, $^3J_{HH}$ = 7.5 Hz), 1.26 (d, 3H, $^3J_{HH}$ = 7.5 Hz), 1.22 (d, 3H, $^3J_{HH}$ = 7.0 Hz), 1.19 (ddd, 1H, $^3J_{HH}$ = 7.0, $^4J_{HH}$ = 2.6, 1.5 Hz), 1.15 (d, 3H, $^3J_{HH}$ = 7.0 Hz), 1.06 (d, 3H, $^3J_{HH}$ = 7.0 Hz) ppm. $^{13}C\{^1H\}$ NMR (C_6D_6, 125 MHz): δ 176.60 (O−C), 167.70 (N═C), 166.00 (N═C), 150.92, 146.89, 139.59, 138.54, 136.14, 125.17, 123.55, 123.20, 122.99, 111.31, 98.03 (═*β*C), 58.45 (−*β*C), 52.40, 51.14, 28.08, 28.02, 27.96, 27.57, 24.14, 23.71, 23.53, 23.41, 23.30, 23.28, 22.88, 22.81, 22.66, 20.18 ppm. Anal. Calcd (%) for $C_{34}H_{48}N_2ONi$: C, 72.99; H, 8.65; N, 5.01. Found: C, 72.93; H, 8.59; N, 4.98.

*Synthesis of $C_{34}H_{48}N_2ONi$, H(BODEI)Ni(η^3-C_3H_5) (**4e**).* A solution of $[(\eta^3\text{-}C_3H_5)NiBr]_2$ (26.9 mg, 0.15 mmol) in THF (2 mL) was added dropwise to a solution of the deprotonated ligand **2** (74.9 mg, 0.15 mmol) in THF (1 mL) at ambient temperature. The color changed from light yellow to orange quickly, and the mixture was stirred at ambient temperature for 1 h. After all the volatiles were removed *in vacuo*, pentane (3 mL) was added. KCl came out immediately and was filtered out. Volatiles of the filtrate were removed *in vacuo* to yield an orange-yellow solid. The crude product was dissolved in minimal pentane, and X-ray quality yellow crystals of **4e** were obtained from slow evaporation of the solvent at −30 °C for several days (27.2 mg, 33% yield). ^1H NMR (C_6D_6, 500 MHz): δ 10.21 (s, 1H), 7.12−7.10 (m, 1H), 7.03−6.96 (m, 5H), 5.64−5.56 (m, 1H), 5.18 (s, 1H), 5.02 (s, 1H), 3.94 (sep, 1H, $^3J_{HH}$ = 7.0 Hz), 3.33 (sep, 1H, $^3J_{HH}$ = 7.0 Hz), 3.29 (sep, 2H, $^3J_{HH}$ = 7.0 Hz), 2.68 (dd, 1H, $^3J_{HH}$ = 6.0, $^4J_{HH}$ = 2.0 Hz), 2.36 (d, 1H, $^3J_{HH}$ = 13.0 Hz), 1.49 (s, 3H), 1.46 (d, 1H, $^3J_{HH}$ = 13.0 Hz), 1.41 (s, 3H), 1.26 (d, 3H, $^3J_{HH}$ = 7.0 Hz), 1.20 (d, 1H, $^3J_{HH}$ = 6.5 Hz), 1.16 (d, 3H, $^3J_{HH}$ = 6.5 Hz), 1.08−1.06 (m, 15H), 1.00 (d, 3H, $^3J_{HH}$ = 7.0 Hz) ppm. $^{13}C\{^1H\}$ NMR (C_6D_6, 125 MHz): δ 176.95 (O−C), 163.34 (N═C), 153.37 (N−C), 151.92, 147.65, 147.56, 140.56, 139.45, 135.27, 124.71, 123.40, 123.24, 123.04, 110.25, 96.50 (═*β*C), 95.93 (═*β*C), 55.20, 51.06, 28.28, 28.22, 27.95, 27.44, 24.84, 24.74, 24.13, 23.88, 23.55, 22.17, 22.12, 19.54 ppm. Anal. Calcd (%) for $C_{34}H_{48}N_2ONi$: C, 72.99; H, 8.65; N, 5.01. Found: C, 70.60; H, 8.16; N, 4.86.

DOI: 10.1021/acs.organomet.6b00256
Organometallics XXXX, XXX, XXX−XXX

*Synthesis of $C_{41}H_{59}N_2OPNi$, H(BODII)Ni(η^1-C_7H_7)PMe$_3$ (**5**).* A solution of (PMe$_3$)Ni(η^3-C_7H_7)Cl (29.2 mg, 0.1 mmol) in toluene (2 mL) was added dropwise to a suspension of the deprotonated ligand **2** (49.9 mg, 0.1 mmol) in toluene (2 mL) at ambient temperature. The suspension became a deep brown solution, and within 10 min KCl precipitation was evident. The mixture was stirred at ambient temperature for 1.5 h. The mixture was then filtered, and all the volatiles of the filtrate were removed *in vacuo* to yield a brown solid. The solid was used without further purification. ^{1}H NMR (C_6D_6, 500 MHz): δ 7.90 (s, 2H), 7.23−6.98 (m, 9H), 5.36 (s, 1H), 4.09 (sep, 2H, $^3J_{HH}$ = 6.5 Hz), 3.27 (s, 2H), 3.09 (sep, 2H, $^3J_{HH}$ = 6.5 Hz), 1.71 (s, 3H), 1.57 (s, 3H), 1.41 (d, 6H, $^3J_{HH}$ = 6.5 Hz), 1.29 (m, 12H), 1.22 (d, 6H, $^3J_{HH}$ = 6.5 Hz), 0.81 (s, 2H), 0.64 (d, 9H, $^2J_{PH}$ = 8.5 Hz) ppm. ^{13}C{^{1}H} NMR (C_6D_6, 125 MHz): δ 173.86 (O−C), 167.47 (N═C), 159.91 (N═C), 146.83, 141.33, 136.23, 129.31, 128.20, 125.46, 123.45, 123.37, 123.04, 122.94, 98.03 (═βC), 53.53 (−βC), 28.06, 28.01, 25.11, 24.42, 24.19, 23.32, 22.85, 19.63, 11.78 (d, $^1J_{PC}$ = 25.1 Hz), 9.35 (d, $^2J_{PC}$ = 31.3 Hz) ppm. ^{31}P{^{1}H} NMR (C_6D_6, 161 MHz): δ −13.60 ppm.

*Synthesis of $C_{38}H_{50}N_2ONi$, H(BODEI)Ni(η^3-C_7H_7) (**6**).* Without purification, crude product **5** and B(C_6F_5)$_3$ (51.3 mg, 0.1 mmol) were dissolved in toluene (2 mL) separately and cooled at −30 °C. B(C_6F_5)$_3$ solution was transferred to the solution of complex **5** dropwise. After being stirred at ambient temperature for 30 min, the volatile of the filtrate was removed *in vacuo* to get a brown solid. Pentane (2 mL) was added to the crude product, and the oil-like brown precipitate stayed insoluble. After being stirred in pentane for 1 h, the precipitate was filtered out and the volatile of the filtrate was removed *in vacuo* to yield **6** as a deep red solid. The product was dissolved in minimal diethyl ether and cooled to −30 °C for several days to yield X-ray quality dark brown crystals (29.7 mg, 51% overall yield). ^{1}H NMR (C_6D_6, 500 MHz): δ 9.55 (s, 1H), 7.12 (t, 1H, $^3J_{HH}$ = 7.3 Hz) 7.11−7.07 (m, 5H), 6.95−6.93 (m, 3H), 6.80−6.78 (m, 3H), 4.95 (s, 1H), 4.84 (s, 1H), 3.92 (sep, 2H, $^3J_{HH}$ = 7.0 Hz), 3.25 (sep, 2H, $^3J_{HH}$ = 7.0 Hz), 1.48 (s, 3H), 1.41 (d, 6H, $^3J_{HH}$ = 7.0 Hz), 1.35 (s, 3H), 1.15 (d, 6H, $^3J_{HH}$ = 7.0 Hz), 1.08 (d, 6H, $^3J_{HH}$ = 6.5 Hz), 1.01 (d, 6H, $^3J_{HH}$ = 7.0 Hz), 0.67 (s, 2H) ppm. ^{13}C{^{1}H} NMR (C_6D_6, 125 MHz): δ 176.34 (O═C), 162.51 (N═C), 152.76 (N−C), 151.94, 147.64, 140.10, 135.03, 132.88, 126.33, 124.69, 123.38, 123.26, 115.79, 107.69, 96.29 (═βC), 96.19 (═βC), 27.89, 27.77, 27.12, 24.01, 23.99, 23.94, 23.39, 19.87 ppm. Anal. Calcd (%) for $C_{38}H_{50}N_2ONi$: C, 74.88; H, 8.27; N, 4.60. Found: C, 70.49; H, 7.75; N, 4.35.

*Synthesis of $C_{35}H_{51}N_2ONi$, H(BODEI)Ni(η^3-C_4H_8) (**7**).* **1** (92.1 mg, 0.2 mmol) and Ni(η^3-methallyl)$_2$ (37.0 mg, 0.22 mmol) were dissolved in toluene (2 mL), heated to 80 °C, and stirred overnight. Afterward, some Ni^0 black precipitate was filtered out, and all the volatiles were removed *in vacuo* to yield **7** as an orange-yellow solid (92.9 mg, 81% yield). X-ray quality, needlelike, yellow crystals were obtained by cooling of a concentrated Et$_2$O solution of **7**. ^{1}H NMR (C_6D_6, 500 MHz): δ 10.31 (s, 1H), 7.13−7.01 (m, 6H), 5.19 (s, 1H), 5.04 (s, 1H), 4.10 (sep, 1H, $^3J_{HH}$ = 6.5 Hz), 3.45 (sep, 1H, $^3J_{HH}$ = 7.0 Hz), 3.38−3.30 (m, 2H) 2.58 (d, 1H, $^4J_{HH}$ = 2.0 Hz), 2.52 (s, 1H), 2.18 (s, 3H), 1.53 (s, 3H), 1.43 (s, 3H), 1.32 (d, 3H, $^3J_{HH}$ = 6.5 Hz), 1.28−1.27 (m, 4H), 1.13−1.10 (m, 16H), 1.00 (d, 3H, $^3J_{HH}$ = 6.5 Hz) ppm. ^{13}C{^{1}H} NMR (C_6D_6, 125 MHz): δ 176.93 (O−C), 163.35 (N═C), 153.19(N−C), 151.79, 147.74, 147.55, 140.79, 139.47, 135.34, 124.65, 123.80, 123.49, 123.26, 123.17, 123.02, 96.56 (═βC), 95.88 (═βC), 65.54, 57.49, 49.08, 28.29, 28.27, 27.93, 27.56, 24.90, 24.79, 24.39, 24.15, 24.02, 23.91, 23.56, 23.20, 22.40, 22.13, 22.00, 19.49, 15.23 ppm. Anal. Calcd (%) for $C_{35}H_{51}N_2ONi$: C, 73.30; H, 8.79; N, 4.88. Found: C, 73.46; H, 8.75; N, 4.89.

*Synthesis of $C_{37}H_{51}N_3ONi$, H(BODEI)Ni(Me)(py) (**8**).* MeLi (0.625 mL, 1.6 M in diethyl ether, 1 mmol) was added dropwise to a stirring suspension of (tmeda)Ni(OAc)$_2$ (146.5 mg, 0.5 mmol) in a 9:1 toluene/THF mixture (5 mL) at −45 °C. The temperature was kept below −25 °C. Once the green suspension turned into a brown-yellow solution, a solution of **1** (138.2 mg, 0.3 mmol) in toluene (1 mL) was added to the mixture at −25 °C followed by an addition of pyridine (0.2 mL, 2.4 mmol). The solution was then heated to 45 °C and stirred for 2 days. Afterward, the mixture was filtered, and the filtrate was concentrated *in vacuo* to less than 1 mL of total volume. A 5 mL amount of pentane was added to precipitate out an orange powder. The mother liquor was decanted out, and the solid was washed by another 5 mL of pentane (118.7 mg, 65% yield). Large X-ray quality brown crystals were obtained by slow diffusion of pentane into a concentrated Et$_2$O solution of **8** at −30 °C. ^{1}H NMR (C_6D_6, 500 MHz): δ 9.25 (s, 1H), 8.88 (d, 2H, $^3J_{HH}$ = 5.0 Hz), 7.13 (s, 3H), 7.02 (m, 1H), 6.88 (s, 1H), 6.87 (s, 1H), 6.25 (t, 1H, $^3J_{HH}$ = 8.0 Hz), 6.03 (t, 2H, $^3J_{HH}$ = 7.0 Hz), 5.23 (1, 1H), 4.95 (s, 1H), 4.17 (sep, 2H, $^3J_{HH}$ = 7.0 Hz), 2.99 (sep, 2H, $^3J_{HH}$ = 6.5 Hz) 1.69 (d, 6H, $^3J_{HH}$ = 6.5 Hz), 1.55 (s, 3H), 1.34 (s, 3H), 1.20 (d, 6H, $^3J_{HH}$ = 7.0 Hz), 0.99 (d, 6H, $^3J_{HH}$ = 6.5 Hz), 0.75 (d, 6H, $^3J_{HH}$ = 6.5 Hz), −0.76 (s, 3H) ppm. ^{13}C{^{1}H} NMR (C_6D_6, 125 MHz): δ 176.03(O−C), 163.08 (N═C), 151.67 (N−C), 150.90, 148.88, 147.27, 141.50, 135.25, 134.82, 127.20, 124.86, 123.29, 123.14, 122.81, 97.85 (═βC), 96.19 (═βC), 28.43, 27.86, 27.69, 25.53, 24.39, 24.03, 24.00, 23.97, 22.98, 22.33, 19.64, −4.77 ppm. Anal. Calcd (%) for $C_{37}H_{51}N_3ONi$: C, 72.55; H, 8.39; N, 6.86. Found: C, 72.14; H, 8.26; N, 6.59.

*Synthesis of $C_{62}H_{86}N_4O_2Ni$, [H(BODII)]$_2$Ni (**9**).* A solution of deprotonated ligand **2** (49.9 mg, 0.1 mmol) in THF (1 mL) was added to a suspension of the Ni(OAc)$_2$ (17.6 mg, 0.1 mmol) in THF (2 mL) at ambient temperature. The suspension became a brown solution, and within 10 min KCl precipitation was evident. The mixture was stirred at ambient temperature for 1 h. All the volatiles were removed *in vacuo*, and *n*-pentane (5 mL) was added to the crude mixture. After stirring in *n*-pentane for 1 h, the mixture was filtered and the filtrate was concentrated and cooled to −30 °C overnight to yield green plate crystals (66.5 mg, 68% yield). ^{1}H NMR (C_6D_6, 500 MHz): δ 7.14−7.08 (m, 6H), 7.04 (d, 2H, $^3J_{HH}$ = 10.0 Hz), 9.69 (d, 4H, $^3J_{HH}$ = 9.5 Hz), 5.43 (s, 2H), 4.01 (sep, 4H, $^3J_{HH}$ = 8.5 Hz), 2.91 (sep, 4H, $^3J_{HH}$ = 8.5 Hz), 2.62 (s, 4H), 1.70 (d, 12H, $^3J_{HH}$ = 8.5 Hz), 1.43 (s, 6H), 1.36 (s, 6H), 1.21 (d, 12H, $^3J_{HH}$ = 8.5 Hz), 1.17 (d, 24H, $^3J_{HH}$ = 8.5 Hz) ppm. ^{13}C{^{1}H} NMR (C_6D_6, 125 MHz): δ 173.16 (O−C), 166.97 (N═C), 166.25 (N═C), 146.58, 144.33, 141.94, 136.18, 125.22, 123.62, 123.24, 123.06, 98.47 (═βC), 49.73 (−βC), 34.15, 28.55, 27.99, 24.30, 23.64, 23.34, 22.78, 22.43, 20.35, 13.98 ppm. Anal. Calcd (%) for $C_{62}H_{86}N_4O_2Ni$: C, 76.14; H, 8.86; N, 5.73. Found: C, 75.83; H, 8.81; N, 5.72.

*Synthesis of $C_{29}H_{36}N_2ONi$, (BKI)Ni(o-tolyl)(py) (**10**).* To a suspension of NaH (35.0 mg, 1.4 mmol) in THF (2 mL) was added dropwise a solution of BKI ligand (259 mg, 1.0 mmol) in THF (3 mL) at ambient temperature. After the gas evolution ceased, the solution was stirred for another 30 min and filtered. A mixture of (tmeda)Ni(*o*-tolyl)Cl (306 mg, 1.0 mmol) and pyridine (0.1 mL) in THF (1 mL) was transferred to the solution at ambient temperature. After being stirred for 1 h, all the volatiles of the mixture were removed *in vacuo*. Hexanes (5 mL) was added to the crude mixture, and the mixture was stirred for another 30 min. The mixture was filtered, and the filtrate was concentrated and cooled to −30 °C overnight to yield orange needlelike crystals (40.6 mg, 42% yield). ^{1}H NMR (C_6D_6, 500 MHz): δ 8.58 (d, 2H, $^3J_{HH}$ = 5.5 Hz), 7.27 (d, 1H, $^3J_{HH}$ = 7.5 Hz), 7.09 (t, 1H, $^3J_{HH}$ = 7.5 Hz), 6.73 (d, 1H, $^3J_{HH}$ = 7.5 Hz), 6.62−6.54 (m, 4H), 6.41 (t, 1H, $^3J_{HH}$ = 7.5 Hz), 6.07 (t, 2H, $^3J_{HH}$ = 7.5 Hz), 5.20 (s, 1H), 4.61 (sep, 1H, $^3J_{HH}$ = 6.5 Hz), 3.75 (s, 3H), 2.88 (sep, 1H, $^3J_{HH}$ = 7.0 Hz), 2.32 (d, 3H, $^3J_{HH}$ = 6.5 Hz) 1.95 (s, 3H), 1.51 (s, 3H), 1.27 (d, 3H, $^3J_{HH}$ = 7.0 Hz), 1.04 (d, 3H, $^3J_{HH}$ = 7.0 Hz), 0.49 (d, 3H, $^3J_{HH}$ = 6.5 Hz) ppm. ^{13}C{^{1}H} NMR (C_6D_6, 125 MHz): δ 176.13 (O−C), 166.71 (N═C), 151.83, 150.91, 148.09, 143.43, 141.41, 141.18, 135.81, 135.18, 125.28, 125.19, 123.25, 123.21, 122.84, 122.25, 121.77, 98.61 (═βC), 28.66, 27.69, 25.79, 25.34, 24.76, 24.62, 24.36, 24.13, 22.85 ppm. Anal. Calcd (%) for $C_{29}H_{36}N_2ONi$: C, 71.48; H, 7.45; N, 5.75. Found: C, 71.34; H, 7.34; N, 5.76.

*Synthesis of $C_{43}H_{54}N_3OLiNi$, Li(BODDI)Ni(o-tolyl)py (**3Li**).* To a solution of **3** (68.9 mg, 0.1 mmol) in Et$_2$O (1 mL) was added dropwise a solution of LiHMDS·Et$_2$O (24.1 mg, 0.1 mmol) in Et$_2$O (2 mL) under stirring at ambient temperature for an hour. Volatiles were removed *in vacuo* to yield a red solid. The crude product was precipitated from a mixture of Et$_2$O (0.1 mL) and pentane (1 mL) cooled to −30 °C overnight, yielding **3Li** as a red precipitate. The

DOI: 10.1021/acs.organomet.6b00256
Organometallics XXXX, XXX, XXX−XXX

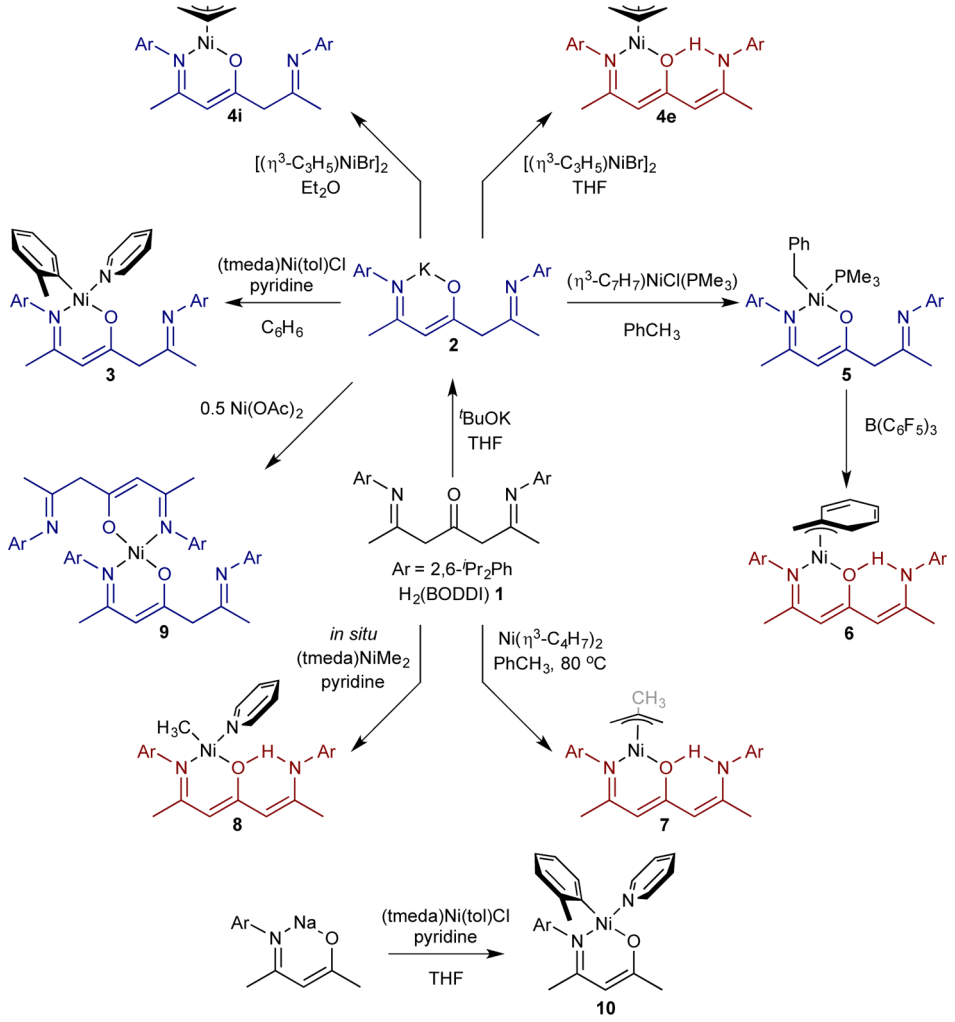

Figure 1. Synthesis of complexes **3**−**10**. Blue ligands indicate the complexes were isolated as the imine tautomer (BODII), while red ligands indicate enamine tautomers (BODEI).

precipitate was recrystallized from pentane (1 mL) again to yield dark red crystals (12.6 mg, 18% yield). X-ray quality brown crystals were obtained in minimal pentane at −30 °C over days. ^{1}H NMR (C_6D_6, 500 MHz): δ 8.70 (br, 1H), 8.09 (br, 1H), 7.71 (d, 1H, $^3J_{HH}$ = 7.5 Hz), 7.04−7.02 (m, 2H, 6.98 (d, 1H, $^3J_{HH}$ = 7.5 Hz), 6.84 (d, 1H, $^3J_{HH}$ = 7.5 Hz), 6.75 (t, 1H, $^3J_{HH}$ = 7.5 Hz), 6.62 (t, 1H, $^3J_{HH}$ = 7.0 Hz), 6.54 (d, 1H, $^3J_{HH}$ = 7.5 Hz), 6.50 (d, 1H, $^3J_{HH}$ = 7.5 Hz), 6.23 (t, 1H, $^3J_{HH}$ = 7.5 Hz), 6.08 (tt, 1H, $^3J_{HH}$ = 7.5, $^4J_{HH}$ = 1.5 Hz), 5.81 (br, 1H), 5.63 (br, 1H), 5.14 (s, 1H), 4.91 (s, 1H), 4.59 (sep, 1H, $^3J_{HH}$ = 6.5 Hz), 3.90 (sep, 1H, $^3J_{HH}$ = 6.5 Hz), 3.57 (s, 3H), 3.08 (sep, 1H, $^3J_{HH}$ = 7.0 Hz), 3.00 (sep, 1H, $^3J_{HH}$ = 6.5 Hz), 1.61 (s, 3H), 1.56−54 (m, 6H), 1.24 (d, 3H, $^3J_{HH}$ = 7.5 Hz), 1.17 (m, 6H), 1.11 (m, 6H), 1.06 (d, 3H, $^3J_{HH}$ = 7.0 Hz), 0.97 (d, 3H, $^3J_{HH}$ = 7.0 Hz) ppm. ^{13}C{^{1}H} NMR (C_6D_6, 125 MHz): δ 170.23(O−C), 164.46 (N═C), 159.16 (N═C), 152.15, 151.63, 148.10, 147.97, 143.79, 143.19, 140.84, 134.90, 134.40, 128.40, 125.15, 124.65, 123.96, 122.81, 122.77, 122.54, 94.35 (═βC), 92.00 (═βC), 27.98, 27.76, 27.59, 27.49, 25.33, 24.90, 24.68, 24.63, 24.56, 24.49, 24.27, 23.86, 23.14, 22.88 ppm. Anal. Calcd (%) for $C_{43}H_{54}N_3OLiNi$: C, 74.36; H, 7.84; N, 6.05. Found: C, 74.17; H, 7.90; N, 6.06.

*Synthesis of $C_{47}H_{64}N_3O_2NaNi$, $(Et_2O)Na(BODDI)Ni(o\text{-}tolyl)py$ (**3Na**).* To a solution of **3** (68.9 mg, 0.1 mmol) in Et_2O (1 mL) was added dropwise a solution of NaHMDS (18.3 mg, 0.1 mmol) in Et_2O (2 mL) while stirring at ambient temperature for an hour. The mixture was concentrated *in vacuo* to a total volume of 1 mL and then cooled −30 °C overnight to yield **3Na** as red needlelike crystals, which were collected via vacuum filtration (62.1 mg, 79% yield). Since coordinated diethyl ether is labile, the crystals were dried *in vacuo* for only another 15 min before being prepared for use. ^{1}H NMR (C_6D_6, 500 MHz): δ 8.40 (d, 2H, $^3J_{HH}$ = 5.0 Hz), 7.42 (d, 1H, $^3J_{HH}$ = 7.0 Hz), 7.08 (d, 2H, $^3J_{HH}$ = 6.5 Hz), 7.01 (t, 2H, $^3J_{HH}$ = 3.0 Hz), 6.86 (t, 2H, $^3J_{HH}$ = 7.0 Hz), 6.63 (d, 1H, $^3J_{HH}$ = 7.0 Hz), 6.35 (t, 1H, $^3J_{HH}$ = 7.0 Hz), 6.27 (t, 1H, $^3J_{HH}$ = 7.0 Hz), 6.16 (t, 1H, $^3J_{HH}$ = 7.5 Hz), 5.81 (br, 2H), 5.25 (s, 1H), 4.91 (s, 1H), 4.28 (br, 2H), 3.70 (s, 3H), 3.21 (q, 4H, $^3J_{HH}$ = 7.0 Hz), 3.05 (br, 2H), 1.71 (s, 3H), 1.68 (s, 3H), 1.27 (d, 6H, $^3J_{HH}$ = 6.5 Hz), 1.23 (br, 18H), 1.07 (t, 6H, $^3J_{HH}$ = 7.0 Hz) ppm. ^{13}C{^{1}H} NMR (C_6D_6, 125 MHz): 173.39 (O−C), 163.64 (N═C), 157.56 (N−C), 152.00, 150.35, 148.57, 145.06, 144.06, 134.28, 134.09, 123.77, 123.20, 122.77, 122.74, 122.67, 122.22, 121.78, 96.73 (═βC), 91.77 (═βC), 65.55, 27.87, 27.26, 24.86, 24.84, 24.74, 24.41, 24.23, 23.47, 22.35, 15.07 ppm. Anal. Calcd (%) for $C_{47}H_{64}N_3O_2NaNi$: C, 71.94; H, 8.22; N, 5.35. Found: C, 68.6; H, 7.18; N, 5.80.

*Synthesis of $C_{86}H_{108}N_6O_2K_2Ni_2$, $[K(BODDI)Ni(o\text{-}tolyl)py]_2$ (**3K**).* To a solution of **3** (68.9 mg, 0.1 mmol) in Et_2O (1 mL) was added dropwise a solution of KHMDS (19.9 mg, 0.1 mmol) in Et_2O (2 mL) under stirring at ambient temperature for an hour. Volatiles were removed *in vacuo* to yield an orange-red precipitate. The product was crystallized by addition of pentane into the crude precipitate, yielding **3K** as orange crystals, which could be collected via vacuum filtration (52.2 mg, 77% yield). The ^{1}H NMR is uninterpretable due to the fluxionality of the structure. After the addition of one equivalent of 18-crown-6, the ^{1}H NMR sharpens considerably. ^{1}H NMR (1 equiv 18c6, C_6D_6, 500 MHz): δ 8.93 (br, 2H), 7.36 (br, 1H), 7.25 (br, 1H), 7.17−7.09 (m, 4H), 7.02 (t, 1H, $^3J_{HH}$ = 7.0 Hz), 6.88 (br, 1H), 6.68 (br,

DOI: 10.1021/acs.organomet.6b00256
Organometallics XXXX, XXX, XXX−XXX

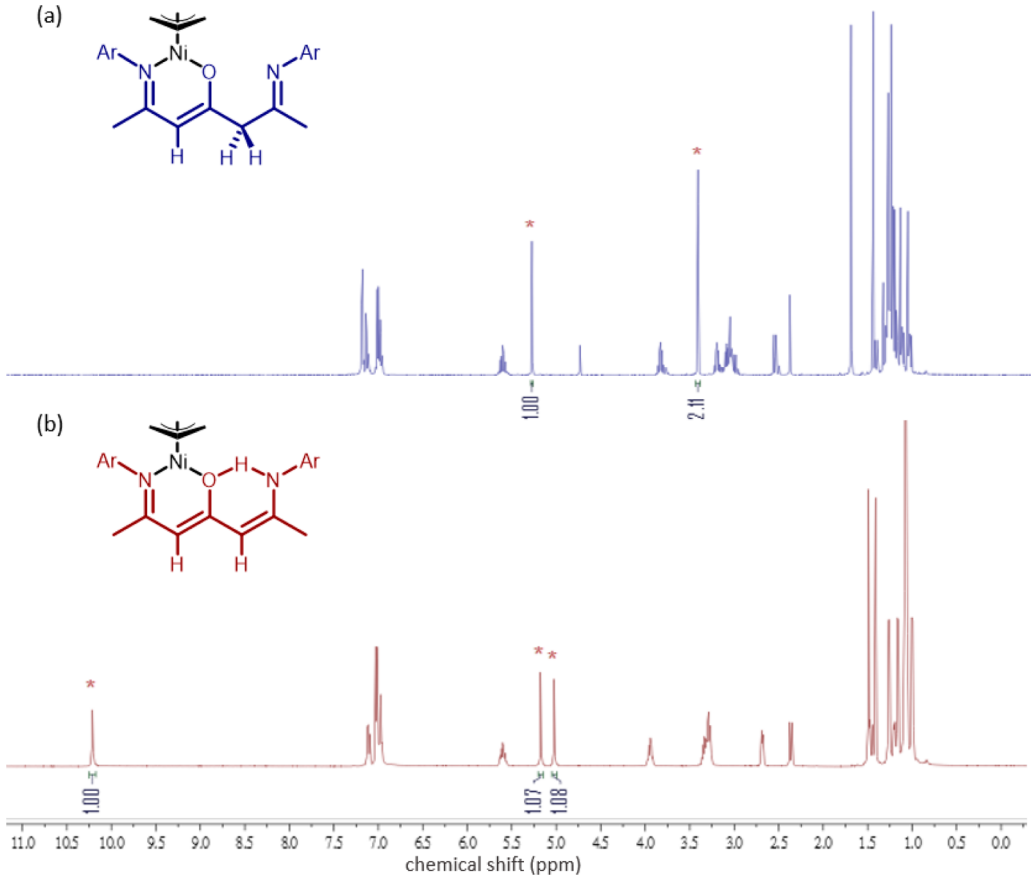

Figure 2. ^{1}H NMR of (a) **4i** with labeled methylene and methine protons and (b) **4e** with labeled methine and enamine protons.

1H), 6.60 (br, 2H), 6.44 (t, 1H, $^3J_{HH}$ = 7.0 Hz), 6.10 (t, 2H, $^3J_{HH}$ = 5.0 Hz), 5.14 (s, 1H), 5.01 (br, 1H), 4.89 (s, 1H), 3.72 (m, 4H), 3.46 (br, 1H), 3.08 (br, 1H), 2.95 (s, 24H), 2.36 (br, 3H), 2.04 (s, 3H), 1.84 (s, 3H), 1.61 (br, 3H), 1.49−1.46 (m, 9H), 0.97 (br, 6H), 0.78 (br, 3H) ppm. Adequate elemental analysis was not obtained for this compound due to residual solvent.

RESULTS AND DISCUSSION

Synthesis and Structural Characterization of Nickel Complexes. Sixteen-electron d^8 square planar H(BODII)Ni and H(BODEI)Ni complexes (H(BODII) = *β*-oxo-*δ*-imineiminato; H(BODEI) = *β*-oxo-*δ*-enamineiminato) were synthesized by salt metathesis or protonolysis, respectively (Figure 1). In the case of the salt metatheses, the protonated ligand H_2(BODDI) (**1**) was deprotonated with ^{t}BuOK to yield the monodeprotonated H(BODII)K salt (**2**), which was then treated with the appropriate Ni halide precursor to yield H(BODII)Ni(*o*-tolyl)(py) (**3**), H(BODII)Ni(η^3-C_3H_5) (**4i**), and H(BODII)Ni(η^3-C_7H_7)(PMe_3) (**5**). Further treatment of **5** with $B(C_6F_5)_3$ yielded the phosphine-scavenged complex H(BODEI)Ni(η^3-C_7H_7) (**6**). For the protonolysis reactions, treatment of **1** with (η^3-C_4H_7)$_2$Ni or *in situ* generated (tmeda)$NiMe_2$[19] yielded H(BODEI)Ni(η^3-C_4H_7) (**7**) and H(BODEI)Ni(Me) (py) (**8**), respectively. Interestingly, attempts to generate **8** via premade (tmeda)$NiMe_2$ were unsuccessful; in the *in situ* reaction, LiCl likely acts as an advantageous Lewis acid that promotes protonolysis. Addition of another Lewis acid, $ZnCl_2$, to the reaction with premade (tmeda)$NiMe_2$ allows for productive reactivity to occur. Upon prolonged standing in solution, **8** slowly decomposes into a bis-ligated species **9**, which can also be independently synthesized via salt metathesis of 2 equiv of **2** with Ni(OAc)$_2$. Finally, a "single-armed" *β*-ketoiminate analogue, **10**, can be prepared by salt metathesis of the deprotonated *β*-ketoiminate ligand with (tmeda)Ni(*o*-tolyl)(py). **10** serves as a control and is similar to a previously reported (*β*-ketoiminate)Ni ethylene polymerization catalyst.[20]

The "free" arm in complexes **3**−**8** could potentially exist as either an imine or enamine. In fact, in virtually all analyses of crude reaction mixtures, *both* tautomers are present. These tautomers are facilely distinguished by ^{1}H NMR: the imine complexes have two singlets with a 2:1 integration ratio for the backbone methylene and methine protons, while the enamine complexes display three singlets in a 1:1:1 ratio for the two backbone methine protons and the enamine proton (Figure 2). In all cases, a single tautomer could be isolated pure from the crude reaction mixture via crystallization.

In the case of complexes **3**−**5** and **9**, which were generated by salt metathesis, the imine tautomer is the major product (95%) of the reaction mixture. While **3** and **5** are mostly insensitive to solvent, complex **4** exhibits a strong solvent dependence on the tautomer ratio: synthesis in Et_2O yields a >95:5 imine:enamine ratio, while synthesis in THF inverts the ratio, yielding 13:87 imine:enamine. This large change in tautomer ratio has allowed for the isolation and structural characterization of both tautomers of **4**, **4i**, and **4e**.

Conversely in the case of **7** and **8**, which were generated by protonolysis, the major tautomer in the crude reaction mixture is the enamine. Similarly, treatment of the imine **5** with $B(C_6F_5)_3$ in toluene to abstract PMe_3 yielded 80% as the enamine tautomer of **6**. Given this result, we questioned

DOI: 10.1021/acs.organomet.6b00256
Organometallics XXXX, XXX, XXX−XXX

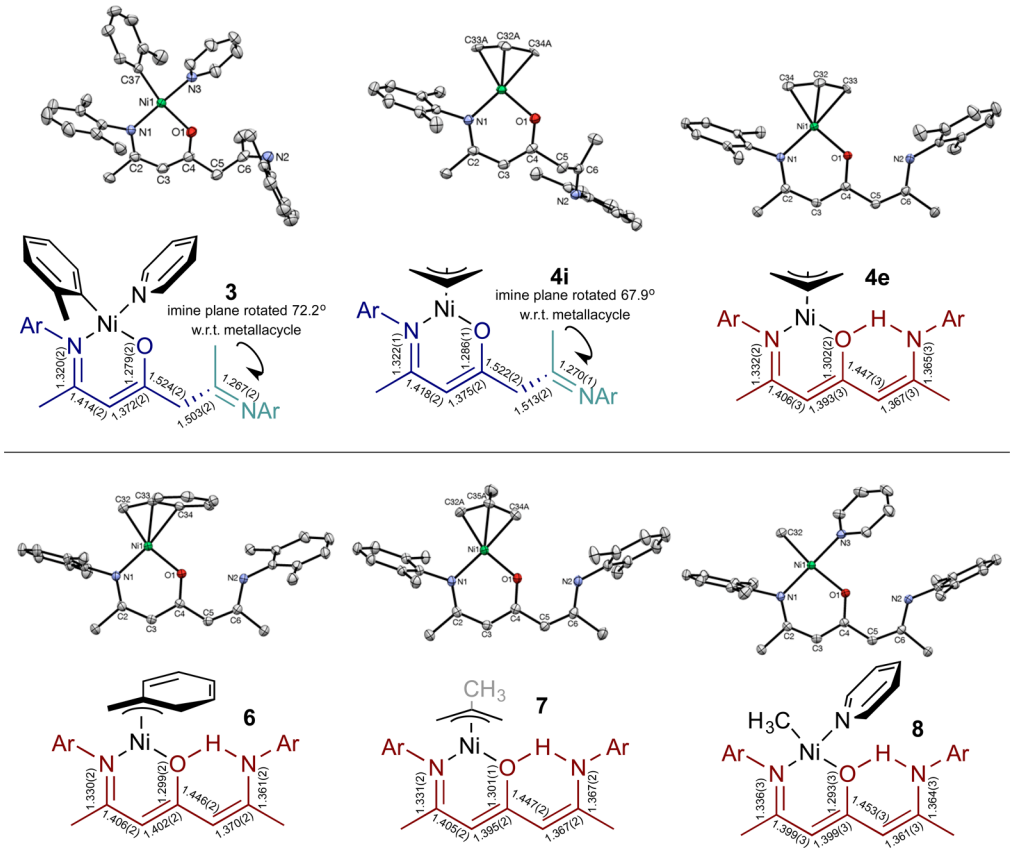

Figure 3. Thermal ellipsoid drawings and bond length cartoons of **3**−**8**. Isopropyl groups have been reduced to the methine carbon, and positional disorder in allyl structures and solvents of crystallization have been removed for clarity. Relevant bond lengths are listed in Table 1.

Table 1. Select Bond Distances (Å) for 3−8, 3Li, 3Na, and 3K

	3	4i	4e	6	7	8	3Li	3Na	3K
Ni−N1	1.896(1)	1.906(1)	1.908(2)	1.899(1)	1.907(1)	1.914(2)	1.956(1)	1.966(1)	1.963(2)
Ni−O1	1.909(1)	1.870(1)	1.863(1)	1.872(1)	1.865(1)	1.932(1)	1.882(1)	1.878(1)	1.854(2)
N1−C2	1.320(2)	1.322(1)	1.332(2)	1.330(2)	1.331(2)	1.336(3)	1.340(2)	1.342(2)	1.336(3)
C2−C3	1.414(2)	1.418(2)	1.406(3)	1.406(2)	1.405(2)	1.399(3)	1.380(2)	1.388(2)	1.393(4)
C3−C4	1.372(2)	1.375(2)	1.393(3)	1.402(2)	1.395(2)	1.399(3)	1.401(2)	1.417(2)	1.413(4)
O1−C4	1.279(2)	1.286(1)	1.302(2)	1.299(2)	1.301(1)	1.293(3)	1.325(2)	1.320(2)	1.327(3)
C4−C5	1.524(2)	1.522(2)	1.447(3)	1.446(2)	1.447(2)	1.453(3)	1.404(2)	1.416(2)	1.412(4)
C5−C6	1.503(2)	1.513(2)	1.367(3)	1.370(2)	1.367(2)	1.361(3)	1.406(2)	1.417(2)	1.424(4)
N2−C6	1.267(2)	1.270(1)	1.365(3)	1.361(2)	1.367(2)	1.364(3)	1.326(2)	1.320(2)	1.315(3)
N2−M							1.915(3)	2.309(1)	2.809(2)
O1−M							1.829(4)	2.242(1)	2.691(2)
C37−M							2.276(6)	2.647(2)	3.091(2)

whether a strong Lewis acid such as $B(C_6F_5)_3$ could affect tautomerization in **3**−**5** or **7**/**8**. Of all of the tested complexes, $B(C_6F_5)_3$ only tautomerized complex **4i** from the imine to the enamine **4e**. Consistent with this observation, quantum chemical structural optimizations at the M06-L/def2-TZVP level[21] predict that the gas-phase free energies of the lowest energy enamine tautomers of **3**, **4**, and **8** are all 0−2.0 kcal/mol lower in energy than corresponding lowest energy imine tautomers. Subsequent single-point calculations at the M06-2X/def2-TZVP level[22] increased this energy difference to 3.4−4.3 kcal/mol, and single-point solvation free energy calculations using the SMD solvation model[23] for diethyl ether found solvent effects to have negligible impact on these free-energy differences. The relatively low sensitivity to functional choice and solvation suggests a consistent, small preference for the enamine over the imine, which is likely attributable to the favorable hydrogen bonding between the enamine N−H and the β-oxygen in the former tautomer. There is no evidence for interconversion between the two tautomers in solution over time (by ^{1}H NMR), under polymerization conditions, or with excess added base (neat pyridine, 500 equiv of NEt_3); all complexes reported herein are kinetically stable.

The solid-state structures of **3**−**8** are presented in Figure 3, and selected bond distances are collected in Table 1. Additional data (including data for **9**) are available in the Supporting Information. The Ni geometry and Ni−L bond distances are typical of those observed in square planar, d^8 16-electron Ni complexes. However, there are significant differences in ligand bond lengths and angles between the imine and enamine tautomers, as illustrated below by **4i** and **4e**. The imine

DOI: 10.1021/acs.organomet.6b00256
Organometallics XXXX, XXX, XXX−XXX

structure **4i** is characterized by a short C6−N2 bond distance (1.270(1) Å) typical of C−N double bonds, long C4−C5 (1.522(2) Å) and C5−C6 (1.513(2) Å) single bonds, and a rotation of the imine π-system 67.9° out plane with respect to the Ni square plane. Conversely, in the enamine structure **4e** the enamine π-system is coplanar with the Ni square plane to facilitate NH−O hydrogen bonding, while the longer C6−N2 bond (1.365(3) Å) and shorter C4−C5 (1.447(3) Å) and C5−C6 (1.367(3) Å) bonds are consistent with π-delocalization across the entire ligand backbone.

Deprotonation of **3** with M(HMDS) (M = Li, Na, K; HMDS = hexamethyldisilazide) yields the bimetallic complexes **3Li**, **3Na**, and **3K** (Figure 4). The crystal structures of **3Li**, **3Na**, and **3K** are presented in Figure 5. The solid-state structures of **3Li** and **3Na** are very similar. In each, the alkali metal sits in the second coordination pocket of the diiminate framework, slightly out of plane with respect to the Ni square plane. Both Na and Li are coordinated to the central O donor and the π-system of the Ni tolyl ligand. The N2−C6, C5−C6, and C4−C5 bond lengths are intermediate when compared to the imine and enamine structures (such as **4i** and **4e**), indicating that the second ligand arm is best described as an anionic enamide conjugated to the Ni N,O chelate (Table 1) with some imine character. Interestingly, the structure of **3K** is a dimeric, bridged structure due to the size of the K atom. In **3K**, the second arm is "flipped" 180° with respect to the Ni N,O chelate, such that K binds only to the δ-N. Instead, the K atom sits significantly farther out of plane of the ligand framework and binds to the tolyl π-system and β-oxygen of a second subunit. This more complicated dimer structure is also evident by NMR: both **3Li** and **3Na** display sharp ^{1}H NMR signals consistent with their sold-state structures, while **3K** displays a broad, fluxional ^{1}H NMR that sharpens only upon addition of an additional ligand such as 18-crown-6. Despite this structural change, the N2−C6, C5−C6, and C4−C5 bond lengths in the enamide arm are similar to those observed in **3Li** and **3Na**.

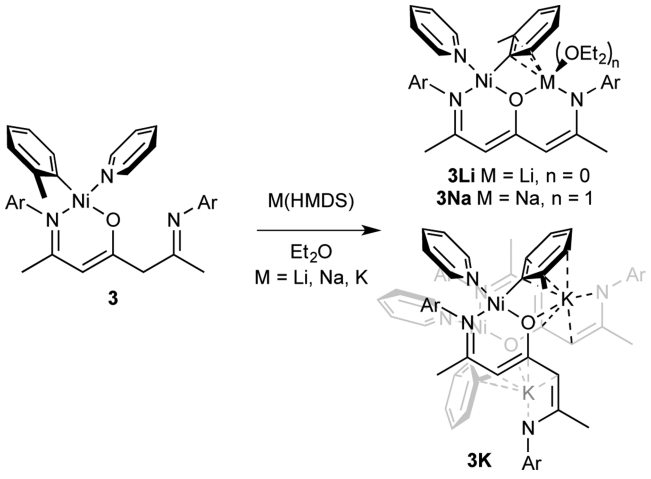

Figure 4. Synthesis of heterobimetallic **3Li**, **3Na**, and **3K** via deprotonation.

Polymerization Behavior. Data for ethylene polymerizations catalyzed by **3**−**8** and **10** are presented in Table 2 and Figure 6. Complexes **3**, **3Li**, **3Na**, **3K**, **8**, and **10** all show moderate polymerization activities (approximately 1×10^5 g/mol/h), while complexes **4i**/**4e**, **6**, and **7** are not active for ethylene polymerization because the η^3-chelates are too stable toward activation by ethylene.[5d,24]

Although they have somewhat similar activities, complexes **3** and **8** show remarkably different polymerization behavior. Upon activation, these two complexes should have tautomeric propagating species (**3** having an imine ligand backbone, **8** having an enamine ligand backbone), and as such, it is possible to interrogate isomer effects on the various steps of polymerization (Figure 7). The imine structure, **3**, yields an order of magnitude higher number-average molecular weight (M_n) polymer than the enamine **8** (12 400 g/mol for **3**, 1600 g/mol for **8**), with a broader molecular weight dispersity $Đ$ (2.6 for **3**, 3.7 for **8**) and less branching (29 branches/1000C for **3**, 118/1000 for **8**). The data for **3** are quite similar to that for the "single-armed" β-ketoiminate analogue **10**, indicating that the pendent imine has little effect on polymerization when compared to the control. Conversely, the enamine **8** exhibits significantly lower M_n and more branching than **3** or **10**.

Given the striking difference in the ethylene polymerization behavior of tautomeric **3** and **8**, we examined ethylene polymerizations catalyzed by **3Li**, **3Na**, and **3K**, anticipating that the now formally anionic enamide side arm would impart more dramatic changes in polymerization behavior. Surprisingly, while polymerizations with **3Li**, **3Na**, and **3K** under standard conditions yielded slightly lower activities, the M_n and $Đ$ values are virtually the same as the imine tautomer **3**. We hypothesize that the deprotonated **3M** catalysts behave more similarly to the imine **3** than the enamine **8** because of rotation around the C4−C5 bond (Figure 8). Upon ethylene insertion into the Ni−tolyl bond, the cation−π interaction to the alkali metal will be weakened/lost, resulting in less preference for the alkali metal to reside in the N,O chelate. Rotation of the C−C bond (as observed in the solid-state structure of **3K**) while maintaining a close ion pair between the enamide and alkali metal would ultimately result in a catalyst structure similar to **3** in overall charge and steric profile.

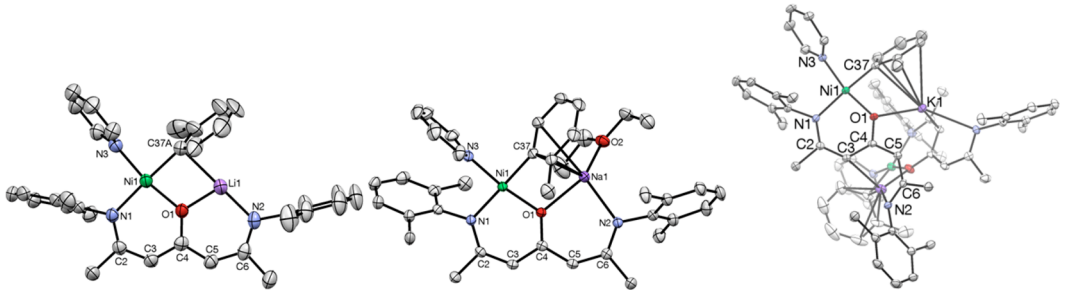

Figure 5. Thermal ellipsoid drawings of **3Li**, **3Na**, and **3K**. Isopropyl groups have been reduced to the methine carbon, and positional disorder in **3Li** structures and solvents of crystallization have been removed for clarity. Relevant bond lengths are listed in Table 1.

DOI: 10.1021/acs.organomet.6b00256
Organometallics XXXX, XXX, XXX−XXX

Table 2. Ethylene Polymerization Data for All Complexes[a]

entry	catalyst	additive/equivalents	yield (mg)	activity (g mol^{-1}h^{-1} × 10^{-5})	M_n (g mol^{-1} × 10^{-4})	$Đ$	branches/1000 C	T_m (°C)	T_c (°C)
1	**3**		215	1.79	1.24	2.56	29	95	82
2	**3**[b]		173	1.44	0.90	2.28	64	84	73
3	**3**	NEt_3/500	199	1.65	1.41	2.26			
4	**4i**		n.d.						
5	**6**		n.d.						
6	**7**		n.d.						
7	**8**		111[c]	0.93	0.16[d]	3.70	118	12	−4
8	**8**	NEt_3/500	104[c]	0.87	0.25[d]	2.88			
9	**10**		144	1.20	1.79	2.36	40	99	87
10	**10**	NEt_3/500	107	0.89	1.80	2.27			
11	**3Li**		117	1.00	1.23	2.58	30	97	86
12	**3Li**	12c4/1	174	1.45	1.15	2.71	47	97	85
13	**3Li**[b]		56	0.47	0.82	2.56	42	76	77
14	**3Li**	NEt_3/500	92	0.68	1.24	2.51			
15	**3Na**		168	1.40	1.49	2.24	41	96	85
16	**3Na**	15c5/1	201	1.67	1.22	2.62	39	96	84
17	**3Na**[b]		52	0.43	0.84	2.38	62	77	76
18	**3Na**	NEt_3/500	113	0.94	1.34	2.45			
19	**3K**		50	0.42	1.12	2.71	43	97	87
20	**3K**	18c6/1	30	0.25	1.24	2.83	32	98	87
21	**3K**[b]		26	0.21	0.84	2.42	39	76	77
22	**3K**	NEt_3/500	37	0.31	1.12	2.83			

[a]Polymerization was run in 2 mL of toluene with catalyst concentrations of 0.2 mM with or without additives at 36 °C under 30 atm of $C_2H_{4(g)}$ for 3 h. Data are an average of 3 runs. [b]The polymerizations were run in THF instead of toluene. [c]Obtained polymers are sticky oils instead of powders. [d]Bimodal distribution was observed. Entries 7 and 8 have a small amount of high molecular weight polymer with an M_n of 3.49 and 3.78 × 10^4 g/mol (5.5% and 7.7%), respectively (Figures S34 and S37).

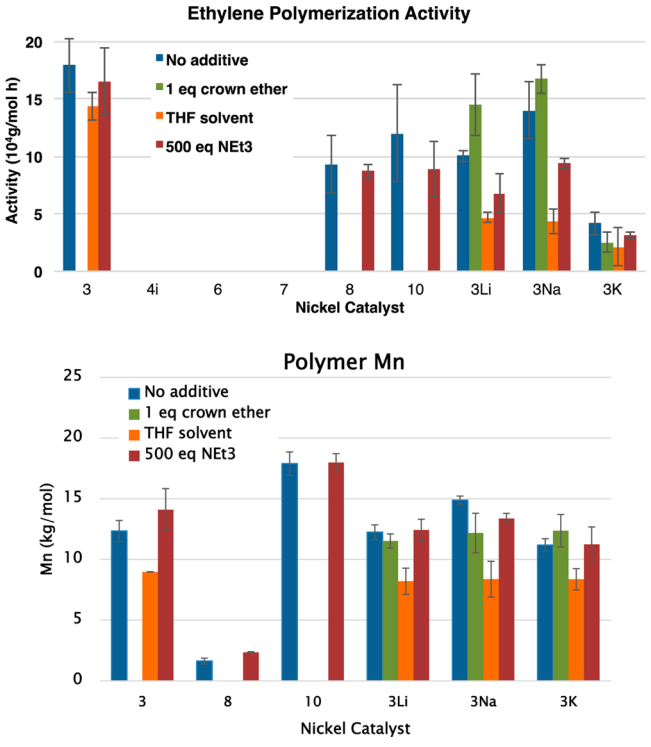

Figure 6. Bar graphs of polymerization activities (top) and polymer M_n (bottom).

In order to test this hypothesis, polymerizations catalyzed by **3**, **3Li**, **3Na**, and **3K** were run in the presence of crown ether (12-crown-4 for Li; 15-crown-5 for Na; 18-crown-6 for K). The crown ether should serve to cap the alkali metal while not fully separating it from the anionic ligand and, thus, should not significantly perturb the overall charge of the active catalyst. In the case where the alkali metal remains in the N,O chelate and also binds the crown, the increased steric pressure on Ni would perturb the rate of β-H elimination/termination as compared to **3**. The results of these polymerization experiments are presented in Table 2. There was little change in polymerization behavior (activity, M_n, or $Đ$) when crown ether additives were used, indicating the capped alkali metal is likely not close to Ni. These results are consistent with the hypothesis that the crown-capped alkali metal complexes behave *as if* they were neutral ligands like **3** with distal enamides rotated out of plane. Conversely, running reactions in THF resulted in a significant drop in polymerization activity for all deprotonated complexes, but not for **3**. We hypothesize that this is the result of a greater

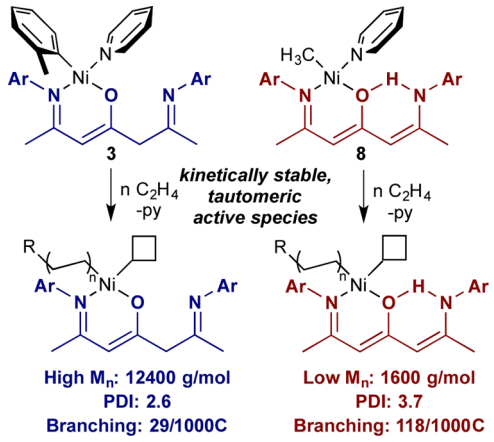

Figure 7. Tautomeric relationship of the active species generated from **3** and **8**.

DOI: 10.1021/acs.organomet.6b00256
Organometallics XXXX, XXX, XXX−XXX

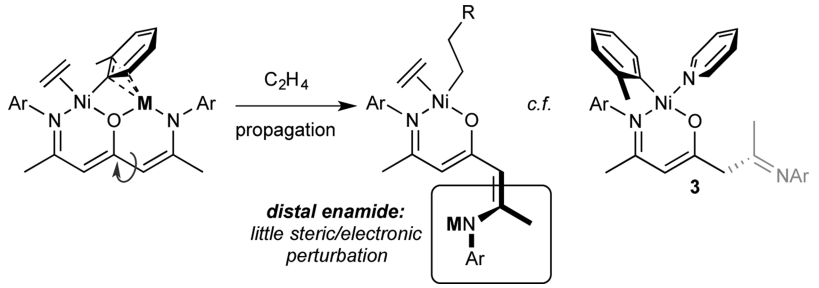

Figure 8. Out-of-plane enamide rotation yields deprotonated active species that are sterically and electronically similar to neutral **3**.

degree of ionization in the polar solvent: the resulting more electron-rich Ni complex would likely yield lower activity.

Finally, all competent polymerization catalysts were tested for their tolerance toward 500 equiv of NEt_3. In all cases, activity remained remarkably high and molecular weight was unchanged, even for the β-ketoiminate single-armed control **10**. These ketoiminate-type complexes are more NEt_3 tolerant than Grubbs-type salicylalidmine catalysts[25] and Agapie's bimetallic catalysts.[7] Unfortunately, none of these complexes catalyze ethylene copolymerization with simple molecules such as 1-octene (standard conditions, 500 equiv of 1-octene) and as such are not candidates for functional comonomer copolymerization. However, these results indicate that a deeper investigation of the functional group tolerance of ketoiminate-type ligands may be warranted.

CONCLUSIONS

A new series of Ni complexes based on a β-oxo-δ-diiminate ligand have been reported. Depending on the method of synthesis and the functional groups on Ni, both enamine and imine tautomers of the ligand have been isolated and characterized. Although the differences in the tautomeric structures are in the second "arm" of the ligand and not in the primary coordination sphere of Ni, they have a large impact on ethylene polymerization catalysis: the enamine tautomer conjugates with the Ni chelate ring and increases electron density on Ni to yield low molecular weight polymers, while the imine tautomer arm rotates out of plane and has minimal influence on polymerization. Installation of an alkali metal in the second coordination pocket of the ligand likewise yields limited influence on polymerization, as the resulting metal enamide "arms" can rotate away from the Ni coordination sphere. Finally, these ketiminate Ni complexes were found to be highly tolerant of NEt_3, warranting further exploration of this class of catalyst in polar olefin polymerization reactions.

ASSOCIATED CONTENT

Supporting Information

The Supporting Information is available free of charge on the ACS Publications website at DOI: 10.1021/acs.organomet.6b00256.

All NMR, XRD, GPC, and DSC data (PDF)
Crystallographic data for **3** (CIF)
Crystallographic data for **4e** (CIF)
Crystallographic data for **4i** (CIF)
Crystallographic data for **6** (CIF)
Crystallographic data for **7** (CIF)
Crystallographic data for **8** (CIF)
Crystallographic data for **3Li** (CIF)
Crystallographic data for **3Na** (CIF)
Crystallographic data for **3K** (CIF)
Crystallographic data for **9** (CIF)
Optimized Cartesian coordinates (XYZ)

AUTHOR INFORMATION

Corresponding Author

*E-mail (I. A. Tonks): itonks@umn.edu.

Notes

The authors declare no competing financial interest.

CCDC entries 1470956−1470965 contain the supplementary crystallographic data for this paper. These data can be obtained free of charge via http://www.ccdc.cam.ac.uk/conts/retrieving.html or from the Cambridge Crystallographic Data Centre, 12 Union Road, Cambridge CB2 1EZ, UK; fax: (+44) 1223-336-033; or e-mail: deposit@ccdc.cam.ac.uk.

ACKNOWLEDGMENTS

We thank the Minnesota Supercomputing Institute (MSI) at the University of Minnesota for providing resources that contributed to the research results reported within this paper. Financial support was provided by the University of Minnesota (start up funds) and the ACS Petroleum Research Fund (ACS-PRF 54225-DNI3). The Bruker-AXS D8 Venture diffractometer was purchased through a grant from NSF/MRI (1224900) and the University of Minnesota. Equipment purchases for the NMR facility were supported through a grant from the NIH (S10OD011952) with matching funds from the University of Minnesota. Victor G. Young, Jr. is thanked for assistance in interpreting XRD data. The authors declare no competing financial interests.

REFERENCES

(1) (a) Britovsek, G. J. P.; Gibson, V. C.; Wass, D. F. *Angew. Chem., Int. Ed.* **1999**, *38* (4), 428−447. (b) Ittel, S. D.; Johnson, L. K.; Brookhart, M. *Chem. Rev.* **2000**, *100* (4), 1169−1204. (c) Gibson, V. C.; Spitzmesser, S. K. *Chem. Rev.* **2003**, *103* (1), 283−316.

(2) (a) Johnson, L. K.; Mecking, S.; Brookhart, M. *J. Am. Chem. Soc.* **1996**, *118* (1), 267−268. (b) Mecking, S.; Johnson, L. K.; Wang, L.; Brookhart, M. *J. Am. Chem. Soc.* **1998**, *120* (5), 888−899. (c) Dai, S.; Sui, X.; Chen, C. *Angew. Chem., Int. Ed.* **2015**, *54* (34), 9948−9953.

(3) (a) Drent, E.; van Dijk, R.; van Ginkel, R.; van Oort, B.; Pugh, R. I. *Chem. Commun.* **2002**, No. 7, 744−745. (b) Carrow, B. P.; Nozaki, K. *Macromolecules* **2014**, *47* (8), 2541−2555.

(4) (a) Weberski, M. P.; Chen, C.; Delferro, M.; Zuccaccia, C.; Macchioni, A.; Marks, T. J. *Organometallics* **2012**, *31* (9), 3773−3789. (b) Stephenson, C. J.; McInnis, J. P.; Chen, C.; Weberski, M. P.; Motta, A.; Delferro, M.; Marks, T. J. *ACS Catal.* **2014**, *4* (3), 999−1003. (c) Wang, J.; Yao, E.; Chen, Z.; Ma, Y. *Macromolecules* **2015**, *48* (16), 5504−5510.

(5) (a) Lee, B. Y.; Bazan, G. C.; Vela, J.; Komon, Z. J. A.; Bu, X. *J. Am. Chem. Soc.* **2001**, *123* (22), 5352−5353. (b) Cai, Z.; Shen, Z.; Zhou, X.; Jordan, R. F. *ACS Catal.* **2012**, *2* (6), 1187−1195.

DOI: 10.1021/acs.organomet.6b00256
Organometallics XXXX, XXX, XXX−XXX

(c) Contrella, N. D.; Jordan, R. F. *Organometallics* **2014**, *33* (24), 7199−7208. (d) Komon, Z. J. A.; Bu, X.; Bazan, G. C. *J. Am. Chem. Soc.* **2000**, *122* (8), 1830−1831.
(6) Cai, Z.; Xiao, D.; Do, L. H. *J. Am. Chem. Soc.* **2015**, *137* (49), 15501−15510.
(7) Radlauer, M. R.; Buckley, A. K.; Henling, L. M.; Agapie, T. *J. Am. Chem. Soc.* **2013**, *135* (10), 3784−3787.
(8) (a) Huang, Y.-B.; Tang, G.-R.; Jin, G.-Y.; Jin, G.-X. *Organometallics* **2008**, *27* (2), 259−269. (b) Takeuchi, D.; Takano, S.; Takeuchi, Y.; Osakada, K. *Organometallics* **2014**, *33* (19), 5316−5323. (c) Zhu, L.; Fu, Z.-S.; Pan, H.-J.; Feng, W.; Chen, C.; Fan, Z.-Q. *Dalton Trans.* **2014**, *43* (7), 2900−2906. (d) Luo, G.; Luo, Y.; Hou, Z.; Qu, J. *Organometallics* **2016**, *35* (5), 778−784.
(9) (a) Ahmed, S. M.; Poater, A.; Childers, M. I.; Widger, P. C. B.; LaPointe, A. M.; Lobkovsky, E. B.; Coates, G. W.; Cavallo, L. *J. Am. Chem. Soc.* **2013**, *135* (50), 18901−18911. (b) Mechler, M.; Latendorf, K.; Frey, W.; Peters, R. *Organometallics* **2013**, *32* (1), 112−130. (c) Mulzer, M.; Tiegs, B. J.; Wang, Y.; Coates, G. W.; O'Doherty, G. A. *J. Am. Chem. Soc.* **2014**, *136* (30), 10814−10820. (d) Bhadra, S.; Akakura, M.; Yamamoto, H. *J. Am. Chem. Soc.* **2015**, *137* (50), 15612−15615.
(10) (a) Baldwin, S. M.; Bercaw, J. E.; Brintzinger, H. H. *J. Am. Chem. Soc.* **2010**, *132* (40), 13969−13971. (b) Hue, R. J.; Cibuzar, M. P.; Tonks, I. A. *ACS Catal.* **2014**, *4* (11), 4223−4231.
(11) (a) Allen, S. D.; Moore, D. R.; Lobkovsky, E. B.; Coates, G. W. *J. Organomet. Chem.* **2003**, *683*, 137−148. (b) Li, S.; Wang, M.; Liu, B.; Li, L.; Cheng, J.; Wu, C.; Liu, D.; Liu, J.; Cui, D. *Chem. - Eur. J.* **2014**, *20* (47), 15493−15498.
(12) Magano, J.; Monfette, S. *ACS Catal.* **2015**, *5* (5), 3120−3123.
(13) Wilke, G. U.S. Patent Appl. US 3422128 A, 1969.
(14) Shim, C. B.; Kim, Y. H.; Lee, B. Y.; Dong, Y.; Yun, H. *Organometallics* **2003**, *22* (21), 4272−4280.
(15) Wilke, G. Google Patents: 1965.
(16) Connor, E. F.; Younkin, T. R.; Henderson, J. I.; Waltman, A. W.; Grubbs, R. H. *Chem. Commun.* **2003**, *18*, 2272−2273.
(17) Gao, H.; Liu, X.; Pei, L.; Wu, Q. *J. Polym. Sci., Part A: Polym. Chem.* **2010**, *48* (5), 1113−1121.
(18) O'Donohue, S. J.; Meehan, E. *Chromatography of Polymers*; American Chemical Society: Washington DC, 1999; Vol. *731*, pp 52−65.
(19) Wiedemann, T.; Voit, G.; Tchernook, A.; Roesle, P. *J. Am. Chem. Soc.* **2014**, *136* (5), 2078−2085.
(20) (a) Song, D.-P.; Ye, W.-P.; Wang, Y.-X.; Liu, J.-Y.; Li, Y.-S. *Organometallics* **2009**, *28* (19), 5697−5704. (b) Song, D.-P.; Shi, X.-C.; Wang, Y.-X.; Yang, J.-X.; Li, Y.-S. *Organometallics* **2012**, *31* (3), 966−975.
(21) Zhao, Y.; Truhlar, D. G. *J. Chem. Phys.* **2006**, *125* (19), 194101.
(22) (a) Weigend, F.; Ahlrichs, R. *Phys. Chem. Chem. Phys.* **2005**, *7* (18), 3297−3305. (b) Weigend, F. *Phys. Chem. Chem. Phys.* **2006**, *8* (9), 1057−1065. (c) Zhao, Y.; Truhlar, D. G. *Theor. Chem. Acc.* **2008**, *120* (1), 215−241.
(23) Marenich, A. V.; Cramer, C. J.; Truhlar, D. G. *J. Phys. Chem. B* **2009**, *113* (18), 6378−6396.
(24) (a) Lee, B. Y.; Bu, X.; Bazan, G. C. *Organometallics* **2001**, *20* (25), 5425−5431. (b) Kim, Y. H.; Kim, T. H.; Lee, B. Y.; Woodmansee, D.; Bu, X.; Bazan, G. C. *Organometallics* **2002**, *21* (15), 3082−3084.
(25) Younkin, T. R.; Connor, E. F.; Henderson, J. I.; Friedrich, S. K.; Grubbs, R. H.; Bansleben, D. A. *Science* **2000**, *287* (5452), 460−462.

DOI: 10.1021/acs.organomet.6b00256
Organometallics XXXX, XXX, XXX−XXX